

37
From: WJ Shack <wjshack@anl.gov> Argonne Nat. Lab
To: Allen Hiser <ALH1@nrc.gov>, Ed Hackett <EMH1@nrc.gov> NRR
Date: 11/4/01 9:47PM
Subject: One last shot

It is probably too late to make any changes in the tech assessment doc, but after the discussion on Friday when I realized that the decision was not whether a 24 month inspection period was acceptable, but rather whether a plant that had not done a credible inspection should inspect now or 6 months from, I wanted to take another look at the more fundamental model that allows initiation at random times and then allows those cracks to grow. Recall that the first nozzle leak at Oconee 3 could well have initiated after about 4 EFPY.

I assumed that initiation of leaks was based on a Weibull model calibrated by field experience, that 0.3 of the leaks lead to circumferential cracks, that the initiated leak (whether from a J groove or an initially axial crack) developed into a 60 degree crack in 3 years. (I could have picked a smaller crack size, but then one gets into discussions of whether the growth is controlled by multiple initiation and growth through the wall or by classical FM controlled growth). However, in addition to the NRC K, I also looked at 3 additional less conservative K distributions.

The calculations with the bounding K acting all 69 nozzles give probabilities that range from 0.39 for Oconee 3 (close to the 95th percentile plants) to 0.02 for other plants. The rate of increase in the CPOF for the 5th, 50th, and 95th percentile plants with this bounding K are 0.04, 0.013, and 0.003 per EFPY.

The two big factors in POF are plant to plant variations (about a factor of 20) and variation with K (about 4 orders of magnitude). In fact the POF changes more than 3 orders of magnitude with a change in K of 4 ksi in^{0.5}.

The variation from plant to plant is real. The variation with K is artificial. It arises from the assumption that all 69 nozzles have the same K. What we don't know and what seems like the highest priority to determine is what fraction of the nozzles have the high Ks and what fraction have low Ks. We will have to see what SIA, Gery, and Richard can do.

There is a kind of threshold behavior that is related to the steep part of the Scott curve. Three of my K distributions which drop the lowest K from 25 to 14 result in a change for Oconee of about a factor of 4 from 0.39 to 0.09. The next drop in the minimum K from 14 to 10 drops the failure probability by orders of magnitude. Conversely it would only take a relatively few high stress nozzles to get Oconee3 up to about 0.1 at 20 EFPY. Most other less susceptible plants would be 0.01 or lower.

B-93

Probability of failure

The probability that a CRDM nozzle will fail at a time t_f less than T , $P(t_f < T)$, can be described as the integral over the operating history of the product of the probability that a crack will initiate at a time t , $p(t)$, and the probability that a crack that initiates at t will fail at a time t_f less than T , $P_c(t_f < T-t)$

$$P(t_f < T) = \int_0^T p(t)P_c(t_f < T-t)dt \quad (3)$$

Equation 3 gives the probability that one tube will fail. If we assume that all N penetrations can be considered as independent, the probability P_N that one of the penetrations will fail at a time $t_f < T$ is

$$P_N = 1 - \prod_{n=1}^N (1 - P_n) \approx \sum_{n=1}^N P_n \quad (4)$$

where N is the total number of penetrations and P_n is the probability of failure of the n th penetration and is small. If it is that the probability of failure of each of the nozzles is the same, then

$$P_N = 1 - (1-P)^N \approx NP \quad (5)$$

for small values of P .

Conditional probability of failure for a growing crack

A conditional probability of failure can be computed for a given crack, if the crack driving force (stress intensity factor) is known as a function of crack size and the distribution of crack growth rates is known. The results presented in Section 6.4.2 on the crack driving force and the crack growth rate distribution described in Section 6.3 have been used to estimate conditional probabilities of failure of throughwall cracks. The development of a reasonable, but conservative distribution for K was discussed in Section 6.4.2. To determine the sensitivity of the results to the assumed K distribution, several other, less conservative distributions for K were considered as shown in Fig. 10. The distributions of K would be expected to vary from nozzle to nozzle, but until more accurate calculations of K for a variety of geometries are available, it is assumed that the distributions shown in Fig. 10 can be used to estimate the sensitivity of the results to the assumed K . Deterministic calculations of the time to failure for variance initial crack sizes for a value of $A=1.8 \times 10^{-11}$ (the 95/50 curve for Alloy 600) are shown in Fig. 11

Once a K distribution is chosen and an initial crack selected the probability $P_c(t_f < T)$ can be determined by fracture mechanics analysis. Because the initial circumferential growth may involve multiple initiations and coalescence of cracks and is difficult to describe analytically although some attempts have been made to deal with this problem,⁶ it was assumed that the fracture mechanics model only governed the growth of the crack after it was greater than 60° in extent. The time taken to grow from initiation of a leak either from a crack in the J groove weld

or by an initially axial crack was taken as a parameter in the model and used in sensitivity studies.

Using the estimate of K in Fig. 10 for the stress intensity, failure calculations were carried out for Alloy 600 nozzles by doing Monte Carlo calculations for the distribution of crack growth rates discussed in Section 6.2. Only the portion of the distribution greater than the 50th percentile was sampled, because field data (Fig. 9) suggests that the heats which are most susceptible to cracking also tend to have higher than average crack growth rates. The resulting conditional cumulative probabilities of failure (CCPOFs) are shown in Fig. 12. Because only the top half of the crack growth distribution is sampled, the curves do not show the strong curvature as the probability approaches 1 that is normally seen in such curves.

Estimates of the probability of failure due to CRDM nozzle cracking

The probability that a crack will initiate at a time t , $p(t)$, in Eq. (3) can be determined using the Weibull probability distribution and the estimates of the Weibull parameters given in Section 6.2. The data given in Section 6.2 are for nozzle leaks. These include leaks due to axial indications as well as circumferential cracks. However, it is only circumferential cracks that are a significant concern in terms of structural integrity and the potential for large amounts of leakage. Only a fraction of the leaks observed to date have been associated with circumferential cracks and the observed data were used to develop a multiplier for the Weibull probabilities to estimate the likelihood of circumferential cracks. Values of the multiplier between 0.2 and 0.3 are consistent with the available data. Sensitivity studies showed that the results did not vary widely for this range of values and the value of 0.3 was used for the reported calculations. The time from initiation to the development of a 60° throughwall crack was varied between 1 and 3 years. The effect of the initiation time is small compared to some other variables and a value of 3 years was used for the reported calculations. This is because of the high variability in failure times associated with corrosion processes that can be characterized by Weibull distributions. In Table 4 the expected times for the first occurrence of a leaking nozzle are shown for several plants for values of the Weibull slope $b=1.5$ and 3. In plants with a large number of nozzle leaks, the first leaks are likely to have occurred many years ago thus a difference of one to two years in the assumed initiation time to transition from an initial leak to a 60° circumferential crack has relatively little impact.

Table 4 Expected times for the first occurrence of a leaking nozzle for Weibull slopes of 1.5 and 3

Plant	EFPY at 600°F	EFPY at 1st initiation	
		b=1.5	b=3
Oconee 3	21.7	4	9
Oconee 2	22	8	13
Oconee 1	21.7	21	21
ANO 1	19.5	19	19
TMI 1	17.5	7	11
Crystal River	15.6	15	15
Surry	16.6	7	11

Realistic estimates of the probability of failure require a knowledge of the distribution of stress intensity for each of the nozzles. Such calculations are not yet available. Using the distribution K1 for all of the nozzles should give very conservative bounding estimates of the cumulative probabilities of failure. Such estimates for several plants and for hypothetical plants at the 5th, 50th, and 95th percentiles of the Weibull shape parameter θ are shown in Table 5. The time dependence of the cumulative probabilities of failure is shown in Fig. 13 for the 5th, 50th, and 95th percentile plants as well as Oconee 3. The slopes of the curves in the region around 20 EFPY give approximately 0.04, 0.013, 0.003 increases in probability of failure per year for the 5th, 50th, and 95th percentile plants.

Table 5 Estimates of the cumulative probability of failure assuming all nozzles have the K1 stress intensity distribution shown in Fig. 10

Plant	EFPY at 600°F	Cumulative POF at EFPY
Oconee 3	21.7	0.39
Oconee 2	22	0.19
Oconee 1	21.7	0.04
ANO 1	19.5	0.03
TMI 1	17.5	0.03
Crystal River	15.6	0.02
Surry	16.6	0.09
95th	20.0	0.02
Median	20.0	0.10
5th	20.0	0.38

The factor of 20 difference between the probabilities of failure between the highest and lowest operating plants reflects that expected between the 5th and 95th percentile plants.

To get insight in the effect of the K distributions on the failure probabilities, the results for Oconee 3 were recalculated for the other stress intensity distributions shown in Fig. 10. The results are summarized in Table 6.

Table 6 Dependence on the cumulative probability of failure of an individual nozzle and a head with 69 nozzles on the K distribution assumed in the failure calculations

K distribution	POF of a nozzle	Cumulative POF
K1	7.2×10^{-3}	0.393
K2	4.4×10^{-3}	0.262
K3	1.4×10^{-3}	0.091

$$\frac{K4 \quad 7.0 \times 10^{-7} \quad 4.8 \times 10^{-5}}{\quad}$$

The four distributions give probabilities of failure that vary about four orders of magnitude. Realistically none of the K distributions will be representative of all the nozzles in a head. More detailed calculations are needed to estimate the fraction of the nozzles that represented by each of the distributions. The probability of failure is likely to be dominated by the number of high stress locations. The probability of failure of n nozzles is almost linear with n as shown in Fig. 14.

Estimates of the probability of failure for an inspection interval

The probability of failure after an inspection is largely governed by the possibility that a large preexisting crack was missed during the inspection interval. The initiation and growth of new cracks appears to be a much smaller contributor to the potential for an failure during an inspection interval. A 165° degree throughwall crack is the largest crack that has been found to date. However, the distributions for K shown in Fig. 10 suggest that the crack will continue to grow once initiated. Thus it is possible that cracks larger than 165° could occur. The variation of the times to reach conditional cumulative probabilities of failure of 0.01 and 0.1 with the initial size of the crack is shown in Fig. 15.

To account for the possibility that larger cracks could be present another set of Monte Carlo calculations were performed. In these calculations a distribution of crack sizes was assumed. Although most leaks have been associated with axial cracks, it was assumed that every leak results in a throughwall circumferential crack with crack sizes that are randomly chosen following the cubic distribution shown in Fig. 16. This distribution provides a conservative estimate for the sizes of all the circumferential cracks that have been observed to date. It gives a probability (≈ 0.1) for large throughwall cracks ($>160^\circ$) that is consistent with current observations, but allows for the potential for cracks greater than 165° in extent. In the calculation the number of leaking nozzles that could occur was determined by sampling from the distribution for the Weibull shape parameter θ given in Section 6.2 and then calculating the resulting number of leaking nozzles at 20 EFPY. The size of the cracks in each nozzle was determined by sampling from the distribution shown in Fig. 16. A crack growth rate for each crack was then determined by sampling from the upper half of the lognormal distribution for crack growth rates given in Section 6.3. The time to failure after 20 EFPY of operation at 600°F was then calculated by determining the minimum time to failure for any of the cracks in the head. The times to failure were ranked order and the probability of failure after a given time determined. The results are shown in Fig. 17. Because these estimates now include the probability that a crack exists, they are actual cumulative probabilities of failure, not conditional failure probabilities as discussed previously. The probabilities of failure shown in Fig. 17 give no credit for the effect of inspections in reducing the probability of failure. The time $t = 0$ corresponds to the time of the inspection.

Table 7 Probability of failure for operation at 318°C for 18 and 24 months after an inspection for which the probability of not detecting a throughwall crack is 0.1

Size distribution	POF	Time to POF
20-330	0.0015	18
20-330	0.0054	24

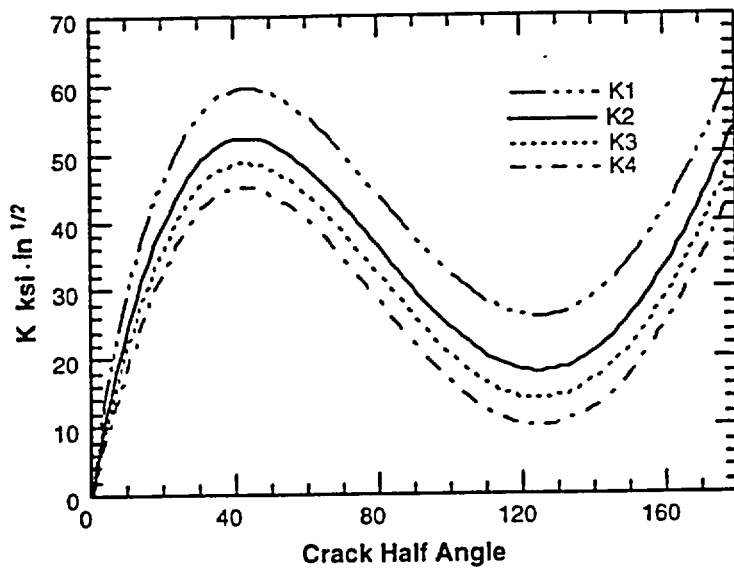


Figure 10. Estimated stress intensity factors K_{est} for a CRDM nozzle. The conservative estimate of K developed in Section 6.4.2 is denoted as $K1$.

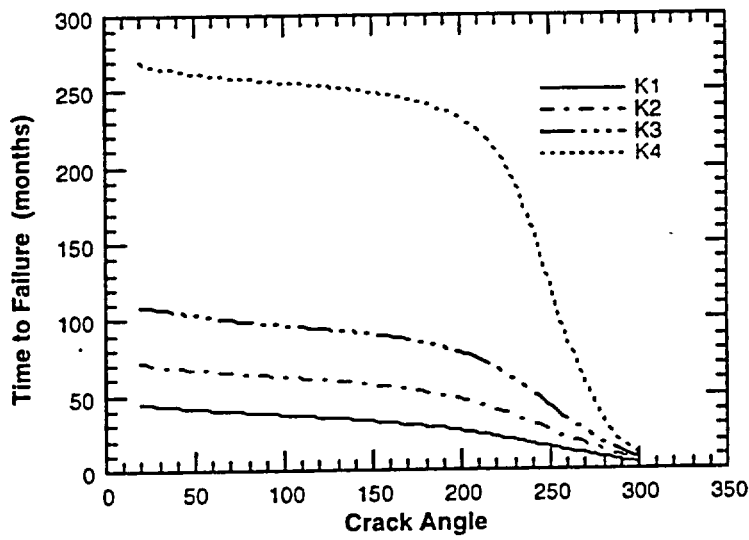


Figure 11. Time to failure for a 95/50 crack growth rate for the 4 stress intensity distributions shown in Fig. 10

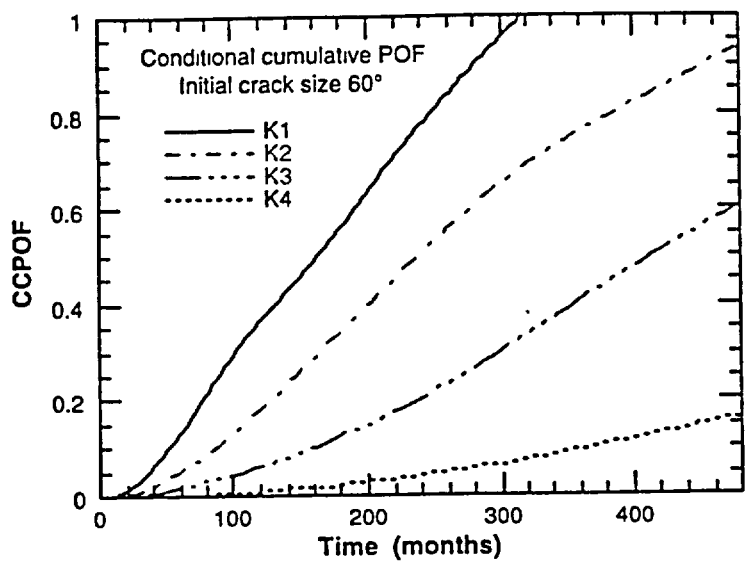


Figure 12.
Conditional probability of failure at 318°C with an initial crack size of 60° using K distributions from Fig. 10

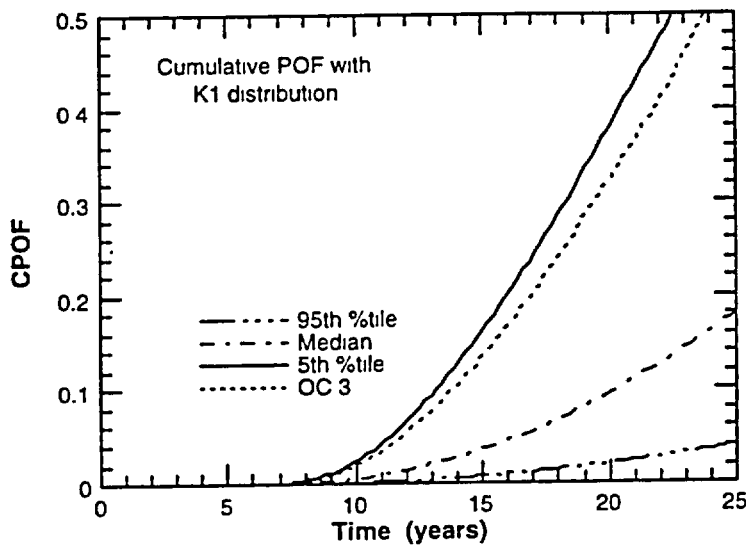


Figure 13.
Variation of the cumulative probability of failure with EFPY assuming all nozzles have the K1 distribution.

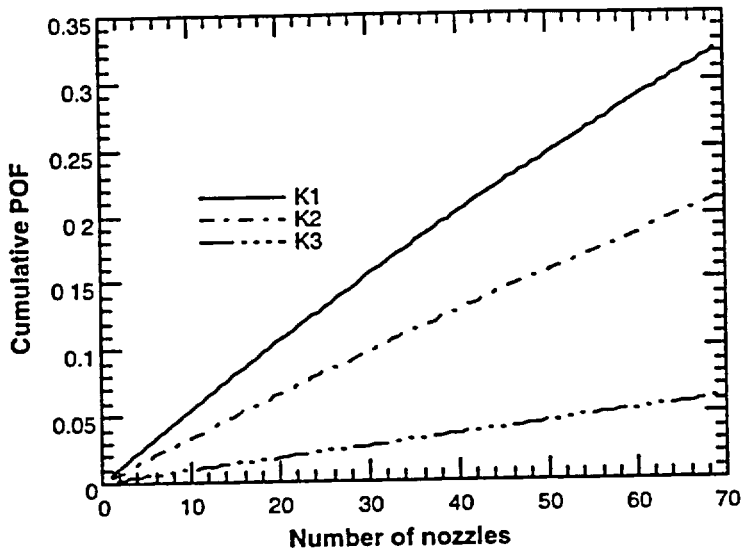


Figure 14. Variation of the cumulative probability of failure at 20 EFY with the number of nozzles characterized by distributions K1, K2, K3. Results for K4 are too low to show.

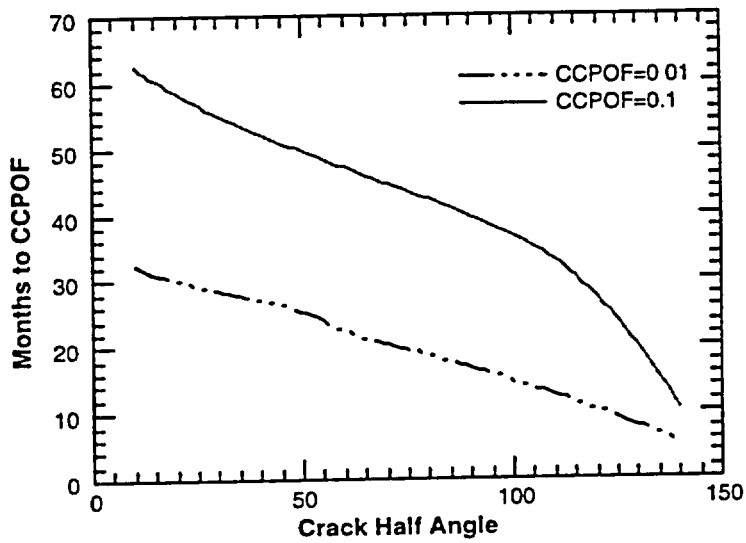


Figure 15. Variation of the time at 318°C to reach a conditional cumulative probabilities of failure of 0.01 and 0.1

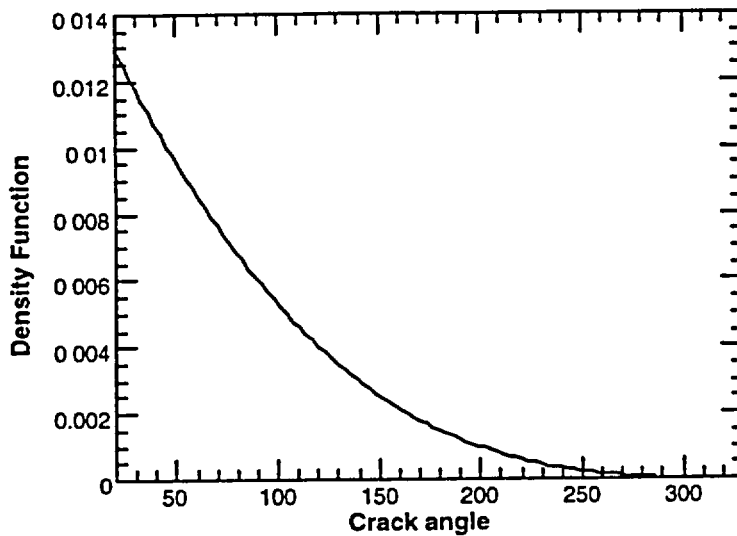


Figure 16.
Density function for the distribution of
initial crack sizes.

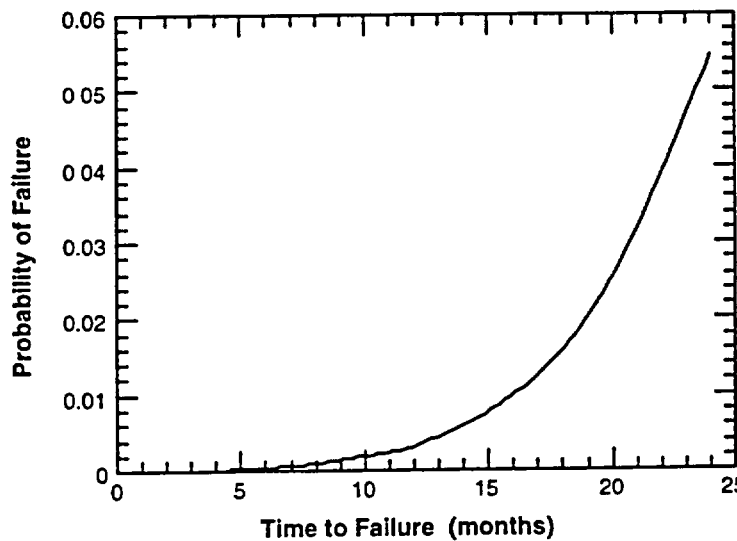


Figure 17.
Probability of failure as function of time
after 20 EFPY of operation for crack size
distributions from 20–330°. No credit is
assumed for inspection.

References

1. P. Scott, Possible Environments responsible for External Surface Cracking of Upper Head Penetrations, Draft Report, EPRI/MRP Experts Group on Alloy 600 and 182 Crack Growth Rates for CRDM Nozzle Cracking, Airlie, Va., October 5–7, 2001.
2. P. Berge, D. Noel, J. M. Gras, and B. Prieux, "Chloride Stress Corrosion Cracking of Alloy 600 in Boric Acid Solutions," *Proc. Eighth International Symposium on Environmental Degradation of Materials in Nuclear Power systems—Water Reactors*, Amelia Island, Fl, American Nuclear Society, LaGrange Park, IL (1997).
3. EPRI TR-104811-V1, *PWR Molar Ratio Control Application Guidelines, Volume 1*, Summary, Electric Power Research Institute, Palo Alto (1995).

4. C. A. Campbell and S. Fyfe, "PWSCC Ranking Model for Alloy 600 Components," *Proc. Sixth International Symposium on Environmental Degradation of Materials in Nuclear Power Systems—Water Reactors*, San Diego, CA, The Minerals, Metals, and Materials Society, Warrendale, PA (1993).
5. G. V. Rao, "Methodologies to Assess PWSCC Susceptibility of Primary Component Alloy 600 Locations Pressurized Water Reactors," *Proc. Sixth International Symposium on Environmental Degradation of Materials in Nuclear Power Systems—Water Reactors*, San Diego, CA, The Minerals, Metals, and Materials Society (TMS), Warrendale, PA (1993).
6. P. Scott, "Prediction of Alloy 600 component failures in PWR systems," *Research Topical Symposia Part 1 - Life Prediction of Structures subject to Environmental Degradation*, National Association of Corrosion Engineers (NACE), Houston, pp 135-160 (1997).
7. Y. S. Garud and R. S. Pathania, "A Simplified Model for SCC Initiation Susceptibility in Alloy 600, with the Influence of Cold Work Layer and Strength Characteristics," *Proc. Ninth International Symposium on Environmental Degradation of Materials in Nuclear Power Systems—Water Reactors*, The Minerals, Metals, and Materials Society (TMS), Warrendale, PA (1999).
8. Z. Szklarska-Smilowska and R. B. Rebak, "Stress Corrosion Cracking of Alloy 600 in High Temperature Aqueous Solutions: Influencing Factors, Mechanisms and Models," in *Control of Corrosion on the Secondary Side of Steam Generators*, Eds. R. W. Staehle, J. A. Gorman, and A. R. McIlree, NACE International, Houston, TX (1996).
9. S. Majumdar, *Assessment of Current Understanding of Mechanism of Initiation, Arrest, and Reinitiation of Stress Corrosion Cracks in PWR Steam Generator Tubing*, NUREG/CR-5752 (2000).
10. G. L. Webb, "Environmental Degradation of Alloy 600 and Welded Filler Metal EN82 in an Elevated Temperature Aqueous Environment," *Proc. Sixth International Symposium on Environmental Degradation of Materials in Nuclear Power Systems—Water Reactors*, San Diego, CA, The Minerals, Metals, and Materials Society (TMS), Warrendale, PA (1993).
11. R. Bandy and D. van Rooyen, "Quantitative Examination of Stress Corrosion Cracking of Alloy 600 In High Temperature Water." *Nuclear Engineering and Design*, v 86 n 1 p 49-56 (Apr 1983).
12. O. K. Chopra, W. K. Soppet, and W. J. Shack, *Effects of Alloy Chemistry, Cold Work, and Water Chemistry on Corrosion Fatigue and Stress Corrosion Cracking of Nickel Alloys and Welds*, NUREG/CR-6721 (2001).
13. P. M. Scott and M. Le Calvar, "Some Possible Mechanisms of Intergranular Stress corrosion Cracking of Alloy 600 in PWR Primary Water," *Proc. Sixth International Symposium on Environmental Degradation of Materials in Nuclear Power Systems—Water Reactors*, San Diego, CA, The Minerals, Metals, and Materials Society (TMS), Warrendale, PA (1993).

14. J. P. Foster, W. H. Bamford, and Raj S. Pathania, "Effect of Materials on Alloy 600 Crack Growth Rates," *Proc. Eighth International Symposium on Environmental Degradation of Materials in Nuclear Power systems—Water Reactors*, Amelia Island, FL, American Nuclear Society, LaGrange Park, IL (1997).
15. J. Foster and W. Bamford, "Alloy 600 Penetration Crack Growth Program," EPRI TR-105406, *Proceedings: 1994 EPRI Workshop on PWSCC of Alloy 600 in PWRs, Part 2*, Licensed Document, Electric Power Research Institute, Palo Alto (1995).
16. T. Cassagne, D. Caron, J. Daret, and Y. Lefevre, "Stress Corrosion Crack Growth Rate Measurements in Alloys 600 and 182 in Primary Water Loops under Constant Load," *Proc. Ninth International Symposium on Environmental Degradation of Materials in Nuclear Power Systems—Water Reactors*, The Minerals, Metals, and Materials Society (TMS), Warrendale, PA (1999).
17. C. Amazallag and F. Vaillant, "Stress Corrosion Crack Propagation Rates in Reactor Vessel Head," *Proc. Ninth International Symposium on Environmental Degradation of Materials in Nuclear Power Systems—Water Reactors*, The Minerals, Metals, and Materials Society (TMS), Warrendale, PA (1999).
18. D. Gómez Briceño and J. Lapeña, "Crack Growth Rates in Vessel Head Penetration Materials," *Proceedings: 1994 EPRI Workshop on PWSCC of Alloy 600 in PWRs, Part 2*, Licensed Document, Electric Power Research Institute, Palo Alto (1995).
19. P. Lidar, M. König, J. Engstrom, and K. Gott, "Effect of Water Chemistry on Environmentally Assisted Cracking in Alloy 600 in Simulated PWR Environments," *Proc. Ninth International Symposium on Environmental Degradation of Materials in Nuclear Power Systems—Water Reactors*, The Minerals, Metals, and Materials Society (TMS), Warrendale, PA (1999).
20. R. W. Staelhe, J. A. Gorman, and K. D. Stavropoulos, *Statistical Analysis of Steam Generator Tube Degradation*, EPRI NP-7493, Licensed Material, Electric Power Research Institute, Palo Alto (1991).
21. V.N. Shah, D.B. Lowenstein, A.P.L. Turner, S.R. Ward, J.A. Gorman, P.E. McDonald, G.H. Weidenhamer, *Nuclear Engineering and Design* **134**, p. 199 (1992).
22. C. Amzallag, F. Vaillant, "Stress corrosion crack propagation rates in reactor vessel head penetrations in Alloy 600," *Proc. Ninth International Symposium on Environmental Degradation of Materials in Nuclear Power Systems—Water Reactors*, The Minerals, Metals, and Materials Society (TMS), Warrendale, PA (1999).